Nowcasting Thunderstorm Anvil Clouds over KSC/CCAFS

David A. Short[1], James E. Sardonia[2], Winifred C. Lambert[1], Mark M. Wheeler[1]

[1]ENSCO, Inc., Cocoa Beach, Florida and

Applied Meteorology Unit, NASA / Kennedy Space Center, Florida

[2]45th Weather Squadron, United States Air Force, Patrick Air Force Base, Florida

Submitted to *Weather and Forecasting*

December 2003

Corresponding Author Address: David A. Short, ENSCO, Inc., 1980 N. Atlantic Ave., Suite 230, Cocoa Beach, Florida, 32931. Email: short.david@ensco.com.

ABSTRACT

Electrified thunderstorm anvil clouds extend the threat of natural and triggered lightning to space launch and landing operations far beyond the immediate vicinity of thunderstorm cells. The deep convective updrafts of thunderstorms transport large amounts of water vapor, super-cooled water droplets and ice crystals into the upper-troposphere, forming anvil clouds, which are then carried downstream by the prevailing winds in the anvil formation layer. Electrified anvil clouds have been observed over the space launch and landing facilities of Kennedy Space Center (KSC) and Cape Canaveral Air Force Station (CCAFS), emanating from thunderstorm activity more than 200 km distant. Space launch commit criteria and flight rules require launch and landing vehicles to avoid penetration of the non-transparent portion of anvil clouds.

The life cycles of 167 anvil clouds over the Florida peninsula and its coastal waters were documented using GOES-8 visible imagery on 50 anvil case days during the months of May through July 2001. Anvil clouds were found to propagate at the speed and direction of upper-tropospheric winds in the layer from 300-to-150 mb, approximately 9.4 km to 14 km, with an effective average transport lifetime of 2 hours and a standard deviation of ~ 30 minutes. The effective lifetime refers to the time required for the non-transparent leading edge of an anvil cloud to reach its maximum extent before beginning to dissipate. The propagation and lifetime information was incorporated into the design, construction and implementation of an objective short-range anvil forecast tool based on upper-air observations, for use on the Meteorological Interactive Data Display System within the Range Weather Operations facility of the 45th Weather Squadron at CCAFS and the Spaceflight Meteorology Group at Johnson Space Center.

1. Introduction

Anvil clouds are formed in the upper troposphere from a supply of water vapor, super-cooled cloud droplets and ice crystals that is carried aloft by the deep convective updrafts of thunderstorms. Of particular interest here are high-level anvil clouds that are generated within an environment with strong vertical wind shear and carried downstream by upper tropospheric winds (Detwiler and Heymsfield 1987). Anvil cirrus is perhaps the most familiar term used for the upper portion of mature and dissipating thunderstorms with *incus*, or anvil, features. However, a variety of terms are in common usage, varying to fit descriptions of the environment and life-history of the system being studied. The following paragraphs are intended to distinguish between some of the more common anvil terms and to clarify how they may relate to the threats of natural and triggered lightning to space launch and landing operations.

The majority of anvil clouds observed in this study showed propagation and lifetime characteristics dominated by moderate to strong upper level shear. In that regard they are similar to the anvils studied by Heymsfield and Blackmer (1988), especially those anvils generated by isolated storms. However the focus of Heymsfield and Blackmer (1988) was on anvil structure, specifically the so-called V feature and thermal couplets in satellite infrared observations associated with severe weather and strong vertical wind shear in the Midwest. Thunderstorm activity associated with strong vertical wind shear also occurs in Florida, westerly shear being correlated with severe weather (Hagemeyer and Schmocker 1991). Easterly shear can also result in high level anvil clouds over the space launch and landing facilities of Kennedy Space Center (KSC) and Cape Canaveral Air Force Station (CCAFS) on Florida's east coast, originating from

convective systems over the Atlantic Ocean. Caniaux et al. (1994) used the term "forward anvil clouds" to describe the westward propagating anvil of a tropical squall line in easterly shear with an easterly jet near 13 km altitude.

Florida also experiences a great deal of thunderstorm activity in low-shear environments, resulting in mesoscale convective complexes with a distinct convective-to-stratiform life cycle (Yuter and Houze 1995). The stratiform portion produces rainfall, a feature not associated with the anvil clouds observed in the present study. The environment of the stratiform portion is generally associated with conditions more restrictive to space launch and landing activities than those posed by non-precipitating anvils. The precipitation, recent and/or nearby thunderstorm activity, and thick cloud layers extending above the freezing level are sufficient to scrub an operation.

Tropical mesoscale convective systems and squall lines can also produce an extensive area of clouds and precipitation behind the active convection. The terms precipitating anvil (Zipser 1977), trailing stratiform anvil (Smull 1995) and *nimbostratus cumulonimbogenitous* (Brown 1979) have been used to describe these precipitating cloud systems.

Braun and Houze (1996) used the term "over-hanging" anvil to describe non-precipitating anvil clouds generated by a Midwest squall line. Low shear environments can produce electrified, overhanging upper level anvil clouds, although their horizontal propagation appears to be limited to a few tens of kilometers from the thunderstorm cells that generated them. Figure 1 shows an example of anvil clouds over the KSC/CCAFS area in a low shear environment, originating from a complex of thunderstorms to the northwest. The SMG post-mission summary for the Space Transportation System

mission 105 (STS-105; the Space Shuttle), reported that although no rain was reported at KSC, thunderstorms were close enough to the Return-To-Launch-Site emergency landing approaches to halt the launch countdown. In addition, the anvil cloud from the thunderstorms had moved overhead of both the SLF and the launch pad violating both the Flight Rules for emergency landings and the Launch Commit Criteria.

Electrified anvil clouds have been observed over the KSC/CCAFS area emanating from thunderstorm activity over the Gulf of Mexico, more than 200 km distant, in environments with strong westerly shear. Mature anvils and even detached anvils can remain electrically charged for several hours, posing the threat of triggered lightning if penetrated by a launch or landing vehicle (Garner et al. 1997). An airborne field mill project (hereafter KSC ABFM 2000) has been designed and conducted to sample electrical fields within thunderstorm anvil clouds in the KSC/CCAFS area and to determine the timescale for decay of the field (Merceret and Christian 2000). The objectives of KSC ABFM 2000 are to provide new information to the Lightning Advisory Panel (Krider et al. 1999) that reviews and formulates natural and triggered lightning Launch Commit Criteria (LCC) for space launch and landing activities.

Charging mechanisms in anvil clouds are complex. However, the general structure is a positively charged center surrounded by negatively charged exterior screening layers near the top and bottom of the anvil cloud (Marshall et al. 1989). The screening layers can have an adverse effect on the ability of the ground-based Launch Pad Lightning Warning System (LPLWS; Harms et al. 1997) to detect electrification in an anvil cloud above the network. Real-time operational decisions are based on an imperative to avoid launch and landing through the optically non-transparent portions of anvil clouds. A

comprehensive set of LCC (Roeder et al. 1999) for space launches of unmanned rockets and the Space Shuttle are used by the 45th Weather Squadron (45 WS) Launch Weather Officers (LWOs) and Flight Rules (FR) are used for the Space Shuttle by the Spaceflight Meteorology Group (SMG). The LCC and FR assure that space flight vehicles remain well clear of such potentially hazardous clouds. The LWOs have identified anvil forecasting as one of their most challenging tasks when attempting to predict the probability of a triggered lightning LCC violation. The goal of the present study was to develop an objective nowcasting technique to determine if the KSC/CCAFS area would be affected by non-transparent anvil clouds.

2. Data and Analysis Procedures

The primary sources of data for this study were images of visible and infrared radiation from the Geostationary Operational Environmental Satellite (GOES), number 8 (GOES-8) and vertical profiles of wind speed, wind direction, temperature and dewpoint from the operational radiosonde network. Lightning data from the Cloud-to-Ground Lightning Surveillance System (CGLSS; Harms et al. 1997) was also used to verify the locations of active thunderstorm cells.

Anvil cloud properties were measured subjectively in an analysis of visible imagery from channel 1 on GOES-8 (0.55-0.75 μm) with a spatial resolution of 1 km. GOES-8 data were archived every 15 to 30 minutes and analyzed using the Man-computer-Interactive-Data-Access-System (McIDAS®; Smith 1975). The McIDAS® software provides the user with customized image enhancement capabilities that facilitate interpretation of cloud features in the satellite imagery. Anvil clouds originating from

small clusters of thunderstorms were readily evident in time loops of visible imagery. These anvil clouds, consistent with the classification *cirrostratus cumulonimbogenitus*, rapidly expanded tens of kilometers or more in a manner consistent with the wind flow in the upper-troposphere, in the layer from about 300 to 150 mb. Down-shear anvil clouds are highly reflective to visible radiation during their growing and mature phases, being composed of ice, primarily in the form of vapor-grown ice crystals and crystal aggregates (Black and Hallett 1998). Such optically non-transparent anvil clouds obscure views of the surface and lower clouds. Infrared imagery (channel 4, 10.2-11.2 μm) indicated radiative temperatures less than 240K at the tops of anvil clouds, consistent with atmospheric temperatures in the upper-troposphere.

An anvil case day was defined as one in which the generation and dissipation of at least three separate anvil clouds was clearly evident and measured from satellite imagery. For the purposes of this study, the life history of an anvil cloud commenced when it first became visible above a thunderstorm complex, and was considered complete when its leading non-transparent edge reached a maximum horizontal distance from the point of origin. Determination of the location of the non-transparent edge was somewhat dependent on the analyst's experience and was subject to an uncertainty estimated to be about 20 km. The uncertainty is a small fraction of the natural variability associated with observed anvils clouds and is not a significant factor in the analysis. At times, anvil-type clouds less than 30-km long were seen in two or three consecutive frames of the GOES-8 visible imagery before dissipating. Fleeting features of this type were associated with isolated thunderstorm cells, consistent with the classification *cirrus spissatus*

cumulonimbogentious, and did not pose the long-range, long-term space-launch and landing threat associated with the anvil clouds included in the analysis presented here.

For each anvil cloud documented in the satellite imagery, the upper tropospheric wind speed, wind direction, temperature and dewpoint from 150 mb to 300 mb were determined from the nearest radiosonde observation that preceded anvil formation. Table 1 lists climatological statistics of the 150 and 300 mb pressure surfaces and the tropopause at the CCAFS balloon facility (ICAO identifier KXMR) for the months of May, June and July. The 150 mb level is the first mandatory level below the average height of the tropopause for the analysis period. The average depth of the 150 to 300 mb layer is 4.4 km. The layer includes the climatological height of the equilibrium level (180 mb) where convective updrafts reach neutral buoyancy, depositing ice crystals, condensation nuclei and water vapor which form the anvil. The average dewpoint depression in the upper tropospheric layer was also determined.

3. Results

Figure 2a shows a scatter diagram of the daily layer-averaged upper-tropospheric wind direction and anvil orientation on 50 case days from May to July 2001, during which 167 anvils were tracked. The diagonal lines indicate the 1:1 line and an envelope of +/- 60 degrees which contains most of the data points. The correlation coefficient between the two variables is 0.97, explaining 94% of the variance. The layer-averaged winds were from the southwest through northwest for most of the case days with a few days showing winds with an easterly component. The average 300-to-150 mb wind direction for the 50 case days was 345°, only one degree greater than the average anvil direction. This indicates that the upper-level wind direction gives a nearly unbiased

indication of anvil orientation. The vast majority of points lie close to the 1:1 diagonal with a few outliers showing discrepancies of more than 60° between the anvil orientation and the upper-level wind direction.

Figure 2b shows the direction difference between the anvil orientation and wind direction as a function of upper tropospheric wind speed. Differences are greatest for lower wind speeds. The standard deviation of differences is about 25° overall, but only about 15° for wind speed greater than 15 ms^{-1}. The dashed lines indicate +/- one standard deviation trends, estimated by a 2nd-order polynomial fit to difference statistics for the three intervals from 0-10, 10-20, and 20-30 ms^{-1}. This result indicates that anvil orientations are more highly correlated with wind direction as the wind speed increases and provides a useful first-guess value for the width of the threat sector described in detail below.

Figure 3a shows a scatter diagram of daily averages of layer-averaged wind speed in the upper-troposphere versus anvil distance for the 50 anvil case days. A linear regression between the two variables gives an intercept of 40 km and a slope of 6.9 km $m^{-1}s$, indicating a time-scale of 6900 seconds = 1.92 hours. With a correlation coefficient of 0.85 the regression relation explains 73% of the variance of anvil distance by the wind speed. This confirms the results of an earlier pilot study that had established a high correlation between upper tropospheric wind speed and anvil transport lifetime (Lambert 2000). The non-zero intercept indicates that anvil clouds can be expected to reach a scale of about 40 km, when the upper-level wind speed is near zero, due to the inertia and divergence of the convective updrafts and their load of hydrometeors.

Figure 3b shows a scatter diagram of wind speed versus anvil length minus the 40 km offset mentioned previously. The solid sloping lines indicate time-scales that are consistent with the wind speeds and anvil distances. For example, a length-offset of 144 km and a speed of 20 m/s indicate a time-scale of 2 hours. The time-scale is referred to as an effective transport lifetime, indicating the approximate time it took the anvil cloud to reach its maximum extent at maturity. The average effective transport lifetime is 1.92 hours with a standard deviation of 0.58 hours.

a. Lower Tropospheric Wind Speed and Direction

Visual inspection of satellite imagery indicated a clear influence of the lower-tropospheric winds on the motion of convective cells and thunderstorms during their developing stages. The average angle between the lower-level winds (900 to 500 mb) and the upper-level winds (300 to 150 mb) was computed at 60° for the 50 anvil case days, with a clockwise rotation with increasing height. However, once an anvil had formed and began to expand, its motion was clearly in accord with the upper-level winds. Therefore, it was concluded that while the lower-tropospheric wind information does provide important clues to the motion of developing convective cells, it does not provide additional information on the subsequent propagation and lifetime of thunderstorm anvil clouds that can be incorporated into an anvil nowcasting technique.

b. Upper Tropospheric Humidity

Figure 4 shows a scatter diagram of dew point depression versus transport lifetime for the 50 anvil case days documented in the present study. A linear regression gives a correlation coefficient of 0.03 and a slope near zero, both of which indicate no useful

relationship between the variables. Nevertheless, it does seem physically plausible that humidity would have an impact on anvil lifetime. This question may be more effectively addressed with an analysis of upper level humidity fields having better spatial and temporal continuity than that provided by the current radiosonde network..

4. Extrapolation/Advection Forecast Tool

The anvil-forecasting tool described below has been implemented on the McIDAS®-based Meteorological Interactive Data Display System (MIDDS) to automatically draw an anvil threat sector on top of an image (satellite or radar composite). In the pre-convective environment the threat sector will alert the forecaster to the specific area where anvils from developing thunderstorms could threaten the launch area within a timeframe of several hours.

The observational studies documented above indicate that the motion of anvil clouds is highly correlated with the speed and direction of upper-level winds. As a result a short-term anvil-forecasting tool can be formulated to extrapolate future positions of anvil clouds as they are advected by the upper-level wind field. By combining data into easily understood information, graphical products help reduce information overload for the meteorologist. If the forecaster expects thunderstorm formation within the threat sector, the anvil clouds from those thunderstorms will likely affect the KSC/CCAFS area and cause violations of the LCC/FR.

Figure 5 shows a schematic representation of an anvil threat sector. The following threat sector properties are consistent with the propagation and lifetime characteristics of thunderstorm anvil clouds observed over Florida and its coastal waters:

- 40 km standoff circle,

- 30 degree sector width,
- Orientation given by 300-to-150 mb average wind direction,
- 1-, 2- and 3- hour arcs in upwind direction, and
- Arc distances given by 300-to-150 mb vector averaged wind speed.

The Applied Meteorology Unit has developed a short-term anvil-forecasting tool for implementation on MIDDS. The tool, activated by a one line McIDAS command, is written in Beginner's All-purpose Symbolic Instruction Code (BASIC) for McIDAS (McBASI) and runs a McBASI script. A "HELP" command for the tool is also available.

Figure 6 shows an example of the anvil threat-sector graphic overlaid on a visible satellite image of the Florida peninsula. The anvil threat sector was computed from radiosonde data observed at KXMR at 1500 UTC (1100 EDT), 13 May 2001, prior to the onset of convective activity. The satellite image was observed at 1915 UTC (1732 local time) just after the onset of convection in central Florida.

Figure 7 shows the anvil threat sector as in figure 6, but for 2132 UTC (1732 EDT). Thunderstorms that formed within the graphical threat sector produced anvil clouds that moved over the KSC/CCAFS area.

5. Summary and Conclusions

The method described herein for the short term prediction of anvil clouds that are generated by thunderstorm activity and advected 10s to 100s of km downstream by upper tropospheric winds was implemented in April 2002 within the Range Weather Operations facility on CCAFS and the SMG at Johnson Space Center to assist forecasters in

nowcasting the threats of natural and triggered lightning to space launch and landing activities at the KSC/CCAFS spaceport. The tool was successfully used to nowcast triggered-lightning threats to the launch of STS-111 on 30 May 2002, which was scrubbed due to encroachment of anvil clouds over the launch complex.

Parameters for the graphical nowcast tool were derived from a study of 167 anvil clouds observed over the Florida peninsula and its coastal waters on 50 case days during May to July 2001. Anvil clouds were found to have an average effective transport lifetime of 2 hours with a standard deviation of about 30 minutes. The distance and direction of propagation was consistent with the average wind speed and wind direction in the layer between 300 and 150 mb, about 9.7 to 14.1 km altitude, just below the tropopause.

The tool has been recently upgraded to include a capability for using forecast upper level winds from the Eta and Rapid Update Cycle models. Possible future work may include an automatic adjustment of the anvil-averaging level for wind speed and direction based on variable thermodynamic considerations such as the equilibrium level and/or the tropopause height.

Notice

Mention of a copyrighted, trademarked or proprietary product, service, or document does not constitute endorsement thereof by the author, ENSCO, Inc., the AMU, the National Aeronautics and Space Administration, or the United States Government. Any such mention is solely to inform the reader of the resources used to conduct the work reported herein.

Acknowledgements

The authors thank Dr. Frank Merceret of the KSC Weather Office for his support of and useful comments on this project.

REFERENCES

Black, R. A., and J. Hallett, 1998: The mystery of cloud electrification. *Amer. Scientist*, **86**, 526-534.

Braun, S. A., and R. A. Houze, Jr., 1996: The heat budget of a mid-latitude squall line and implications for potential vorticity production. *J. Atmos. Sci.*, **53**, 1217-1240.

Brown, J. M., 1979: Mesoscale unsaturated downdrafts driven by rainfall evaporation: A numerical study. J. Atmos. Sci., **36**, 313-338.

Caniaux, G., J.-L. Redelsperger, and J.-P. Lafore, 1994: A numerical study of the stratiform region of a fast-moving squall line. Part I: General description and water and heat budgets. *J. Atmos. Sci.*, **51**, 2046-2074.

Detwiler, A. and A. J. Heymsfield, 1987: Air motion characteristics in the anvil of a severe thunderstorm during CCOPE. *J. Atmos. Sci.*, **44**, 1899-1911.

Garner, T., R. Lafosse, D. G. Bellue, and E. Priselac, 1997: Problems associated with identifying, observing, and forecasting detached thunderstorm anvils for Space Shuttle operations. Preprints, *7th Conference on Aviation, Range, and Aerospace Meteorology*, Long Beach, CA, Amer. Meteor. Soc., 302-306.

Hagemeyer, B. C., and G. K. Schmocker, 1991: Characteristics of East-Central Florida tornado environments. *Wea. Forecasting*, **6**, 499-514.

Heymsfield, G. M., and R. H. Blackmer, Jr., 1988: Satellite-observed characteristics of Midwest severe thunderstorm anvils. *Mon. Wea. Rev.*, **116**, 2200-2224.

Harms, D. E., B. F. Boyd, R. M. Lucci, M. S. Hinson, and M. W. Maier, 1997: Systems used to evaluate the natural and triggered lightning threat to the Eastern Range and Kennedy Space Center. Preprints, *28th International Conference on Radar Meteorology*, Austin, TX, Amer. Meteor. Soc., 240-241.

Krider, E. P., H. C. Koons, R. L. Walterscheid, W. D. Rust, and J. C. Willett, 1999: Natural and Triggered Lightning Launch Commit Criteria (LCC). Prepared by The Aerospace Corporation, El Segundo CA 90245, Aerospace Report TR-99(1413)-1; Prepared for Space and Missile Systems Center, 2430 E. El Segundo Blvd., Los Angeles AFB, CA 90245, SMC Report SMC-TR-99-20. 15 pp.

Lambert, W. C., 2000: Improved anvil forecasting: Phase I Final Report. NASA Contractor Report CR-2000-208573, Kennedy Space Center, FL, 24 pp. [Available from ENSCO, Inc., 1980 N. Atlantic Ave., Suite 230, Cocoa Beach, FL, 32931.]

Marshall, T. C., W. D. Rust, W. P. Winn, and K. E. Gilbert, 1989: Electrical structure in two thunderstorm anvil clouds. *J. Geophys. Res.*, **94**, 2171-2181.

Merceret, F.J. and H. Christian, 2000: KSC ABFM 2000 - A Field Program to Facilitate Safe Relaxation of the Lightning Launch Commit Criteria for the American Space Program. Preprints, *9th AMS Conference on Aviation and Range Meteorology*, Orlando, FL, Amer. Meteor. Soc., 447-449.

Roeder, W. P., J. E. Sardonia, S. C. Jacobs, M. S. Hinson, D. E. Harms, and J. T. Madura, 1999: Avoiding triggered lightning threat to space launch from the Eastern Range/Kennedy Space Center, Preprints, *8th Conference on Aviation, Range, and Aerospace Meteorology*, Dallas, TX, Amer. Meteor. Soc., 120-124.

Smith, E. A., 1975: The McIDAS system. *IEEE Trans. GeoSci. Electron.*, **GE-13**, 123-136.

Smull, B. F., 1995: Convectively induced mesoscale phenomena in the tropical and warm-season midlatitude atmosphere. Reviews of Geophysics, Supplement, U.S. National Report 1991-1994, pp. 897-906.

Yuter, S. E., and R. A. Houze, Jr., 1995: Three-dimensional kinematic and microphysical evolution of Florida cumulonimbus. Part I: Spatial distribution of updrafts, downdrafts, and precipitation. *Mon. Wea. Rev.*, **123**, 1921-1940.

Zipser, E. J., 1977: Mesoscale and convective-scale downdrafts as distinct components of squall line structure. *Mon. Wea. Rev.*, **105**, 1568-1589.

Figure Captions

Fig. 1. A GOES-8 visible image at 2115 UTC (1715 EDT) on the afternoon of 9 August 2001. Anvil clouds that forced the STS-105 launch to be postponed can be seen over the Cape Canaveral area (center of the image), emanating from a thunderstorm complex to the northwest.

Fig. 2. Daily anvil orientation versus wind direction in panel (a) and deviation of anvil orientation from wind direction versus wind speed in panel (b). Note that the deviations are largest at the lowest wind speeds. The dashed lines in (b) indicate +/- one standard deviation trends, estimated from difference statistics for the three intervals from 0-20, 20-40, and 40-60 kts.

Fig. 3. Daily averages of wind speed versus anvil distance in panel (a) and daily averages of wind speed versus anvil distance minus offset in panel (b). The 21 nm offset used in (b) was determined from the linear regression in (a). The sloping lines in (b) denote effective transport lifetimes, calculated from the ratio of distance-offset to wind speed.

Fig. 4. Daily averages of dew point depression versus transport lifetime for the 50 anvil case days observed during May through July 2001. Transport lifetimes were derived from the analysis shown in Figure 3b. The solid line was determined by linear regression.

Fig. 5. Schematic representation of an anvil threat sector. The sector is 30° in width, extending toward the southwest from a 20 n mi circle centered on the station of interest. Arcs are located upstream at distances consistent with 1-, 2- and 3-hour transport times by the upper-level winds.

Fig. 6. An example of the anvil forecast graphic overlaid on a visible satellite image of the Florida peninsula. The anvil threat corridor was computed from radiosonde data observed at XMR at 1500 UTC (1100 EDT), 13 May 2001, prior to the onset of convective activity. The satellite image was observed at 1915 UTC (1732 local time) just after the onset of convection in central Florida.

Fig. 7. As in figure 6, but for 2132 UTC (1732 EDT). Thunderstorms that formed within the graphical threat sector produced anvil clouds that moved over the KSC/CCAFS area.

Table Captions

Table 1. Climatological pressures and heights of the tropopause, 300 mb surface and 150 mb surface at KXMR for the months of May, June and July.

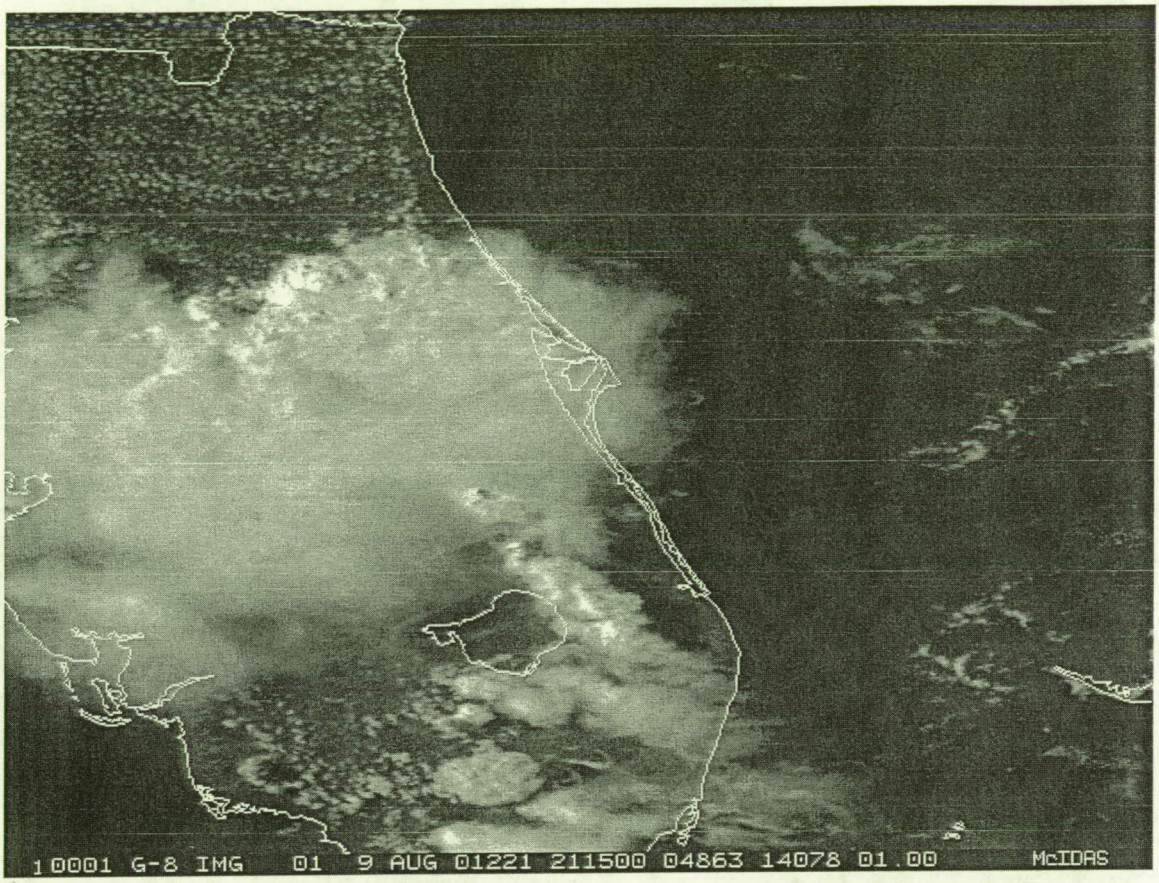

Fig. 1. A GOES-8 visible image at 2115 UTC (1715 EDT) on the afternoon of 9 August 2001. Anvil clouds that forced the STS-105 launch to be postponed can be seen over the Cape Canaveral area (center of the image), emanating from a thunderstorm complex to the northwest.

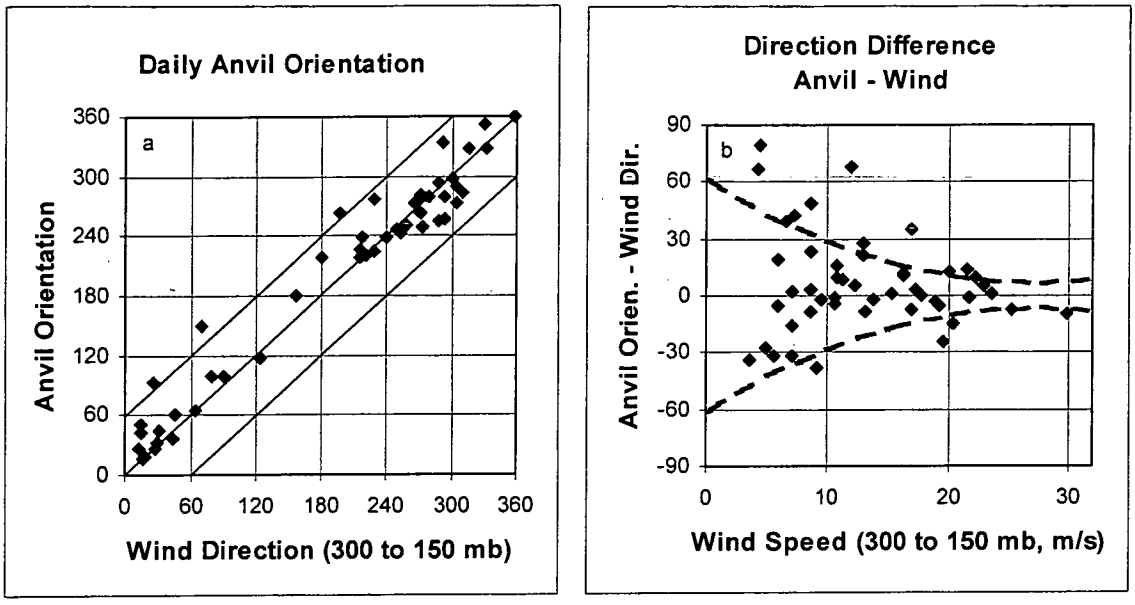

Fig. 2. Daily anvil orientation versus wind direction in panel (a) and deviation of anvil orientation from wind direction versus wind speed in panel (b). Note that the deviations are largest at the lowest wind speeds. The dashed lines in (b) indicate +/- one standard deviation trends, estimated from difference statistics for the three intervals from 0-20, 20-40, and 40-60 kts.

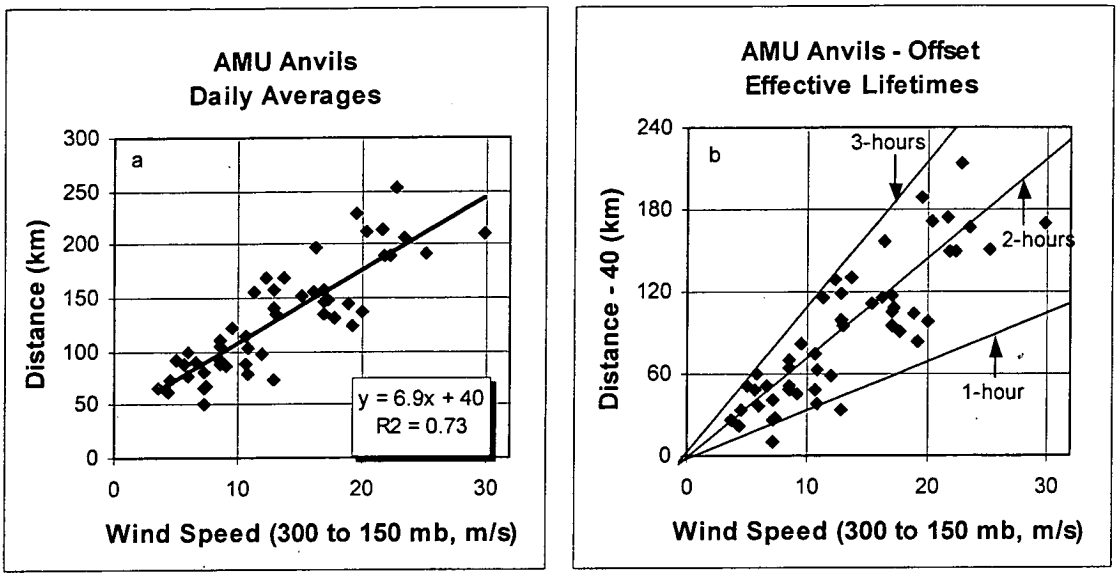

Fig. 3. Daily averages of wind speed versus anvil distance in panel (a) and daily averages of wind speed versus anvil distance minus offset in panel (b). The 40 km offset used in (b) was determined from the linear regression in (a). The sloping lines in (b) denote effective transport lifetimes, calculated from the ratio of distance-offset to wind speed.

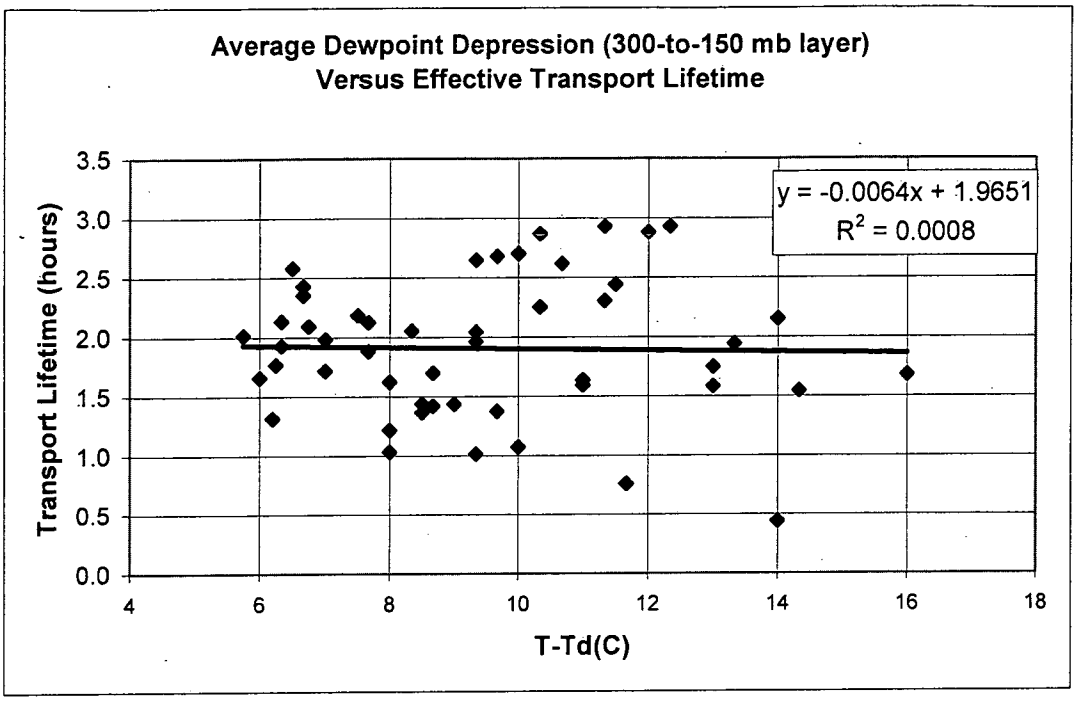

Fig. 4. Daily averages of dew point depression versus transport lifetime for the 50 anvil case days observed during May through July 2001. Transport lifetimes were derived from the analysis shown in Figure 3b. The solid line was determined by linear regression. In these cases the 300-to-150 mb dewpoint depression was not a good predictor of anvil transport lifetime.

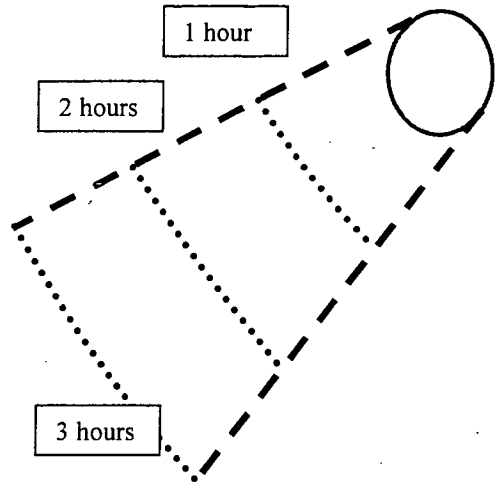

Fig. 5. Schematic representation of an anvil threat sector. The sector is 30° in width, extending toward the southwest from a 40 km circle centered on the station of interest. Arcs are located upstream at distances consistent with 1-, 2- and 3-hour transport times by the upper-level winds. If thunderstorms are forecast within the threat sector, their anvil clouds will likely enter the circle around the station of interest and will arrive within a time interval indicated by the arcs.

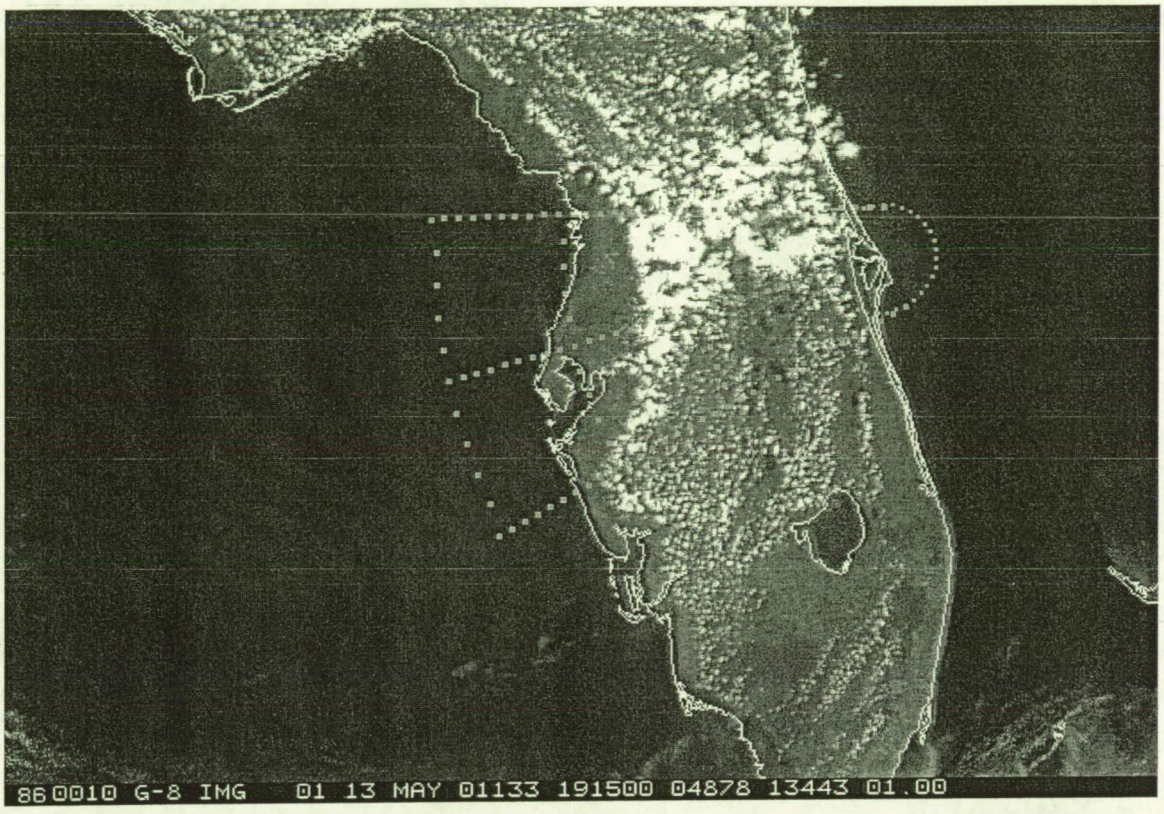

Fig. 6. An example of the anvil forecast graphic overlaid on a visible satellite image of the Florida peninsula. The anvil threat corridor was computed from radiosonde data observed at KXMR at 1500 UTC (1100 EDT), 13 May 2001, prior to the onset of convective activity. The satellite image was observed at 1915 UTC (1732 local time) just after the onset of convection in central Florida.

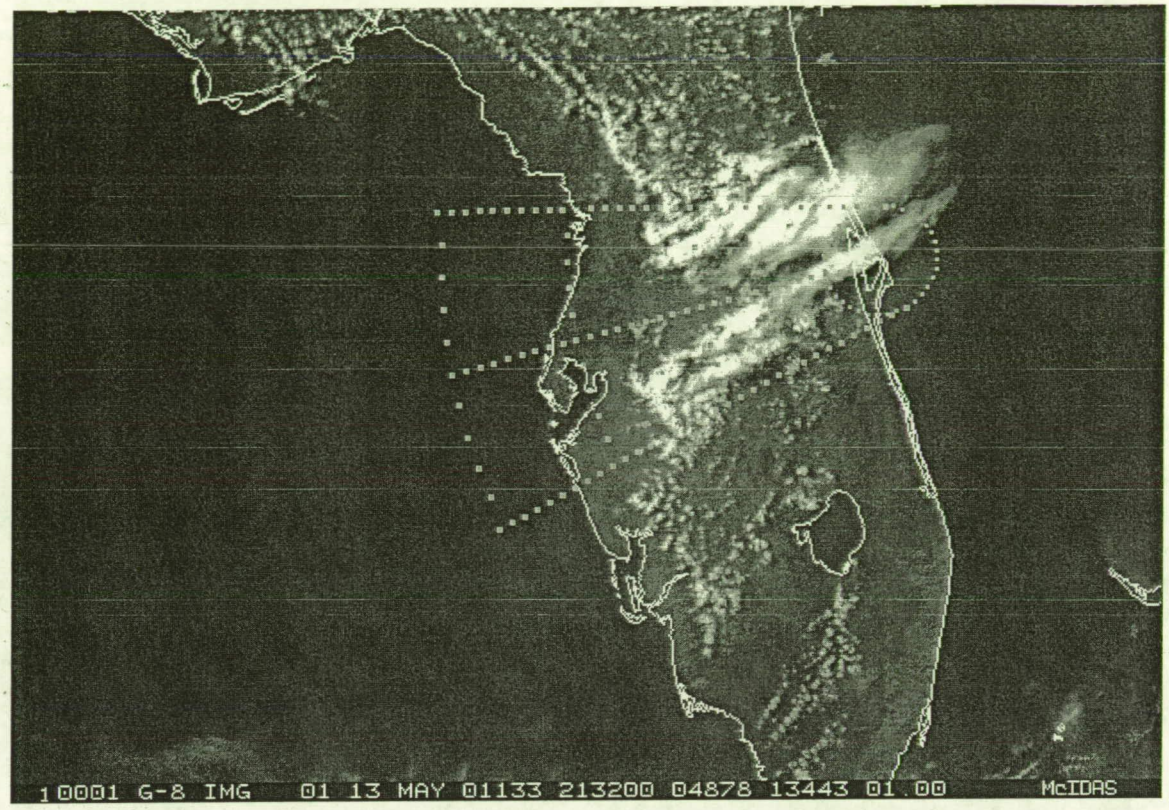

Fig. 7. As in figure 6, but for 2132 UTC (1732 EDT). Thunderstorms that formed within the graphical threat sector produced anvil clouds that moved over the KSC/CCAFS area.

Tables

Table 1. Climatological pressures and heights of tropopause, 300 mb surface and 150 mb surface at KXMR for the months of May, June and July. The climatology was developed from a 20-year database 1973-to-1992 by the Range Commanders Council Meteorology Group. See the following website: http://www.edwards.af.mil/weather/rcc.htm

Month	***Tropopause Pressure (mb)***	***Tropopause Height (km)***	***150 mb Height (km)***	***300 mb Height (km)***	***150 to 300 mb Thickness (km)***
May	142	14.5	14.0	9.6	4.4
June	129	15.1	14.1	9.7	4.4
July	128	15.1	14.2	9.7	4.5